6-9-1959

A Numerical Solution for Weak Disturbances in a Large Scale Hydromagnetic Field

Patrick J. Blewett

A NUMERICAL SOLUTION - BLEWETT

NAME AND ADDRESS	DATE

A NUMERICAL SOLUTION FOR WEAK DISTURBANCES IN A LARGE SCALE HYDROMAGNETIC FIELD

By

Patrick J. Blewett

A Thesis

Submitted in Partial Fulfillment of the

Requirements for the Degree of

Master of Science in Physics

The University of New Mexico

1959

This thesis, directed and approved by the candidate's committee, has been accepted by the Graduate Committee of the University of New Mexico in partial fulfillment of the requirements for the degree of

MASTER OF SCIENCE

E. F. Castetter
DEAN

June 9, 1959
DATE

Thesis committee

Donald J. Skubelman
CHAIRMAN

C. P. Leavitt

Jack Katzenstein

Elsasser[1] has shown that the equations of magnetohydrodynamics for an ideal, incompressible, unbounded, perfectly conducting fluid in a magnetic field may be put in the symmetrized form

$$\frac{\partial \vec{p}}{\partial t} + (\vec{q}\cdot\nabla)\vec{p} + \nabla\psi = 0$$

$$\frac{\partial \vec{q}}{\partial t} + (\vec{p}\cdot\nabla)\vec{q} + \nabla\psi = 0$$

$$\nabla\cdot\vec{p} = \nabla\cdot\vec{q} = 0 \qquad (1)$$

where

$$\vec{p} = \vec{V} + \vec{B}^*$$
$$\vec{q} = \vec{V} - \vec{B}^*$$
$$\psi = \frac{p}{\rho} + \frac{(\vec{p}-\vec{q})^2}{8}$$
$$\vec{B}^* = (\mu\rho)^{-\frac{1}{2}}\vec{B}. \qquad (2)$$

$\vec{V}$, p, ρ, and $\vec{B}$ are respectively the fluid velocity, the pressure, the density, and the magnetic induction vector.

Letting

$$\vec{p}_0(\vec{r},t) = \vec{V}_0 + \vec{B}_0^*$$
$$\vec{q}_0(\vec{r},t) = \vec{V}_0 - \vec{B}_0^*$$
$$\psi_0 = \frac{p_0}{\rho} + \frac{(\vec{p}_0-\vec{q}_0)^2}{8} \qquad (3)$$

be a solution of (1) and thus the primary hydromagnetic field, Skabelund[2] has shown that superimposed perturbations,

$$\vec{\tilde{p}} = \vec{\tilde{V}} + \vec{\tilde{B}}^*$$
$$\vec{\tilde{q}} = \vec{\tilde{V}} - \vec{\tilde{B}}^* \qquad (4)$$

---

1. Elsasser, Phys. Rev. 79, 183 (1950)

2. Skabelund, O.N.R. Tech. Rep. 17, Contr. 1288(00), (1955)

on the primary field also satisfy (1). They are related to the primary field in Lagrangian coordinates by

$$\vec{\tilde{P}} = (\vec{\tilde{P}}^{\circ} \cdot \nabla^{\circ})\vec{r} \tag{5}$$

$$\nabla \cdot \vec{\tilde{P}} = \nabla^{\circ} \cdot \vec{\tilde{P}}^{\circ} = 0 \tag{5}$$

where r is an integral of

$$\frac{d\vec{r}}{dt} = \vec{Q}_0(\vec{r}, t). \tag{6}$$

Note, the superscript o's denote initial values: the quantities with tildes constitute the superimposed waves on the primary field which is denoted by the subscript o's. Further, in the above analysis $\vec{\tilde{Q}}$ was assumed small compared to $\vec{\tilde{P}}$ which condition yielded the relation

$$\frac{\partial \vec{\tilde{P}}}{\partial t} = \nabla \times (\vec{Q}_0 \times \vec{\tilde{P}}). \tag{7}$$

From this equation it is seen[3] that the lines of $\vec{\tilde{P}}$ are frozen in a hypothetical incompressible fluid moving with velocity, $\vec{Q}_o$. Hence, from equation (3b) we see that if the actual fluid's velocity is 0, the Q_o-fluid flows with a velocity, $-\vec{B}^*_o$; whereas, when the actual fluid moves with velocity, $\vec{V}_o$, the velocity of the Q_o-fluid is increased to $\vec{V}_o - \vec{B}^*_o$.

Strictly speaking, equations (5) and (7) hold only in the absence of reflections; however, Skabelund argues their reasonableness in the presence of reflections provided the amplitude of $\vec{\tilde{P}}$ is small compared to the amplitude of $\vec{Q}_o$.

---

3. Prandtl and Tietjens, Fundamentals of Hydro and Aero-Mechanics (McGraw-Hill, New York, 1934), p. 197

and the scale of $\vec{\tilde{P}}$ remains small compared to the scale of $\vec{Q}_o$. By scale is meant the linear distance in any direction over which the relative change in the variable is unity.

Our concern here will be to investigate the form of certain solutions of equation (7); we will be content with a two dimensional analysis. Following Skabelund, $\vec{Q}_o$ is expanded in a Taylor's series

$$\vec{Q}_o(x,y) = \vec{Q}_o(x_o y_o) + \left(\frac{\partial \vec{Q}_o}{\partial x}\right)_{x_o y_o}(x - x_o) + \left(\frac{\partial \vec{Q}_o}{\partial y}\right)_{x_o y_o}(y - y_o). \tag{8}$$

From equation (1d) Q_o is solenoidal, hence

$$\nabla \cdot \vec{Q}_o(x,y) = \left(\frac{\partial Q_{ox}}{\partial x}\right)_{x_o y_o} + \left(\frac{\partial Q_{oy}}{\partial y}\right)_{x_o y_o} = 0. \tag{9}$$

Let

$$a = \left(\frac{\partial Q_{ox}}{\partial x}\right)_{x_o y_o} \qquad b = \left(\frac{\partial Q_{ox}}{\partial y}\right)_{x_o y_o}$$

$$c = \left(\frac{\partial Q_{oy}}{\partial x}\right)_{x_o y_o} \qquad d = \left(\frac{\partial Q_{oy}}{\partial y}\right)_{x_o y_o} \tag{10}$$

and from equation (9)

$$a + d = 0. \tag{11}$$

Thus, the first order approximation in component form becomes

$$Q_{ox} = K_1 + ax + by$$

$$Q_{oy} = K_2 + cx - ay \tag{12}$$

where for convenience we take x_o and y_o as 0, and

$$K_1 = Q_{ox}(0,0)$$

$$K_2 = Q_{oy}(0,0). \tag{13}$$

The streamlines of the Q_o-fluid are the curves satisfying

$$\frac{q_{oy}}{q_{ox}} = \frac{dy}{dx} = \frac{K_2 + cx - ay}{K_1 + ax + by}. \qquad (14)$$

Considering this equation in the form,

$$(K_2 + cx - ay)\,dx - (K_1 + ax + by)\,dy = 0 \qquad (15)$$

we see that it is exact; its solution is the general equation of a conic

$$\frac{c}{2}x^2 - \frac{b}{2}y^2 - axy + K_2 x - K_1 y + e = 0 \qquad (16)$$

having the discriminant

$$\Delta = a^2 + bc. \qquad (17)$$

Consider first the elliptical case wherein $\Delta < 0$, or

$$a^2 + bc < 0. \qquad (18)$$

We will insure this condition by taking

$$a = 0,\ b > 0,\ c < 0. \qquad (19)$$

There is no loss of generality here since the mixed term in (16) could always be eliminated through the proper rotation of axes. Hence, we have for the streamlines for the case of elliptical flow of our imaginary Q_o-fluid the equation

$$\frac{c}{2}x^2 - \frac{b}{2}y^2 + K_2 x - K_1 y + e = 0. \qquad (20)$$

For the solution of $\vec{P}$ in equation (7), our final goal, we see from (5) that we will need a Lagrangian description of

The generalization of the [illegible]

$$\frac{\partial \varphi_y}{\partial \varphi_x} = \frac{dy}{dx} = \frac{[illegible]}{[illegible]}$$

Considering this equation in the form,

$$[illegible] = 0$$

we see that it is exactly [illegible] equa-

tion of a conic

$$[illegible] = 0$$

having the discriminant

$$\Delta = a^2 + bc.$$

1.4 Consider first the elliptical [illegible]

$$a^2 + bc < 0.$$

We will insure this condition by taking,

$$a = 0,\ b > 0,\ c < 0.$$

There is no loss of generality [illegible]

in (16) could always be eliminated [illegible]

tion of axes. Hence, we [illegible]

case of elliptical flow of [illegible]

tion

$$[illegible] \qquad (19)$$

For the solution of [illegible]

see from (9) that we will need [illegible] the Q_o-fluid flow. For this we return to equation (6) from which

$$\dot{x} = Q_{ox}(\vec{r}, t)$$

$$\dot{y} = Q_{oy}(\vec{r}, t) \qquad (21)$$

and from the equations of expansion, (12), we have

$$\dot{x} = K_1 + by$$

$$\dot{y} = K_2 + cx \qquad (22)$$

from which

$$\ddot{x} = b[K_2 + cx]$$

$$\ddot{y} = c[K_1 + by] \qquad (23)$$

This pair of equations then yields the solutions

$$x = Ce^{\sqrt{bc}\,t} + De^{-\sqrt{bc}\,t} - \frac{K_2}{c}$$

$$y = Ae^{\sqrt{bc}\,t} + Be^{-\sqrt{bc}\,t} - \frac{K_1}{b}. \qquad (24)$$

Equations (24) are subject to the initial conditions

$$t = 0: \qquad x = x^o \qquad \dot{x} = K_1 + by^o$$

$$y = y^o \qquad \dot{y} = K_2 + cx^o. \qquad (25)$$

These conditions are sufficient for the determination of the integration constants in equations (24). The result is

$$x = \sqrt{\frac{b}{c_1}}\left[y^o + \frac{K_1}{b}\right]\sin\sqrt{bc_1}\,t - \sqrt{\frac{b}{c_1}}\left[\frac{K_2}{\sqrt{bc_1}} - \sqrt{\frac{c_1}{b}}\,x^o\right]\cos\sqrt{bc_1}\,t + \frac{K_2}{c_1}$$

$$y = \left[y^o + \frac{K_1}{b}\right]\cos\sqrt{bc_1}\,t + \left[\frac{K_2}{\sqrt{bc_1}} - \sqrt{\frac{c_1}{b}}\,x^o\right]\sin\sqrt{bc_1}\,t - \frac{K_1}{b} \qquad (26)$$

where $c_1 = -c$ and thus, $c_1 > 0$. Equations (26) are the equations of motion of the Q_o-fluid in Lagrangian coordinates.

That they constitute the parametric equations for an elliptic trajectory of a particular Q_o-fluid particle can be seen by noting

$$x = \sqrt{\frac{b}{c_1}}\left[E\sin\theta - F\cos\theta\right] + \frac{K_2}{c_1}$$

$$y = E\cos\theta + F\sin\theta - \frac{K_1}{b} \tag{27}$$

where the substitutions are easily recognized. From (27) then

$$\frac{\left[y + \frac{K_1}{b}\right]^2}{E^2+F^2} + \frac{\left[x - \frac{K_2}{c_1}\right]^2}{\frac{b}{c_1}\left[E^2+F^2\right]} = 1. \tag{28}$$

Thus, we have for the paths of the various Q_o-fluid particles ellipses centered about $(\frac{K_2}{c_1}, \frac{-K_1}{b})$ with an eccentricity

$$e = \sqrt{1 - \frac{c_1}{b}}\,. \tag{29}$$

The following graph, figure 1, will help to visualize the flow of particles which constitute the positive x axis when $t = 0$. For calculation purposes it was assumed that

$$K_1 = K_2 = 0\,, \quad \frac{b}{c} = -2. \tag{30}$$

Now with equations (26) and (5) $\vec{P}$ can be determined for an arbitrary small-amplitude initial distribution. Rewriting equation (5a) in component form

$$\tilde{P}_x = \tilde{P}_x^o \frac{\partial x}{\partial x^o} + \tilde{P}_y^o \frac{\partial x}{\partial y^o}$$

$$\tilde{P}_y = \tilde{P}_x^o \frac{\partial y}{\partial x^o} + \tilde{P}_y^o \frac{\partial y}{\partial y^o} \tag{31}$$

and substituting equations (26) into the above yields

$$\tilde{P}_x = \tilde{P}_x^o \cos\sqrt{bc_1}\,t + \tilde{P}_y^o \sqrt{\frac{b}{c_1}} \sin\sqrt{bc_1}\,t$$

$$\tilde{P}_y = -\tilde{P}_x^o \sqrt{\frac{c_1}{b}} \sin\sqrt{bc_1}\,t + \tilde{P}_y^o \cos\sqrt{bc_1}\,t \tag{32}$$

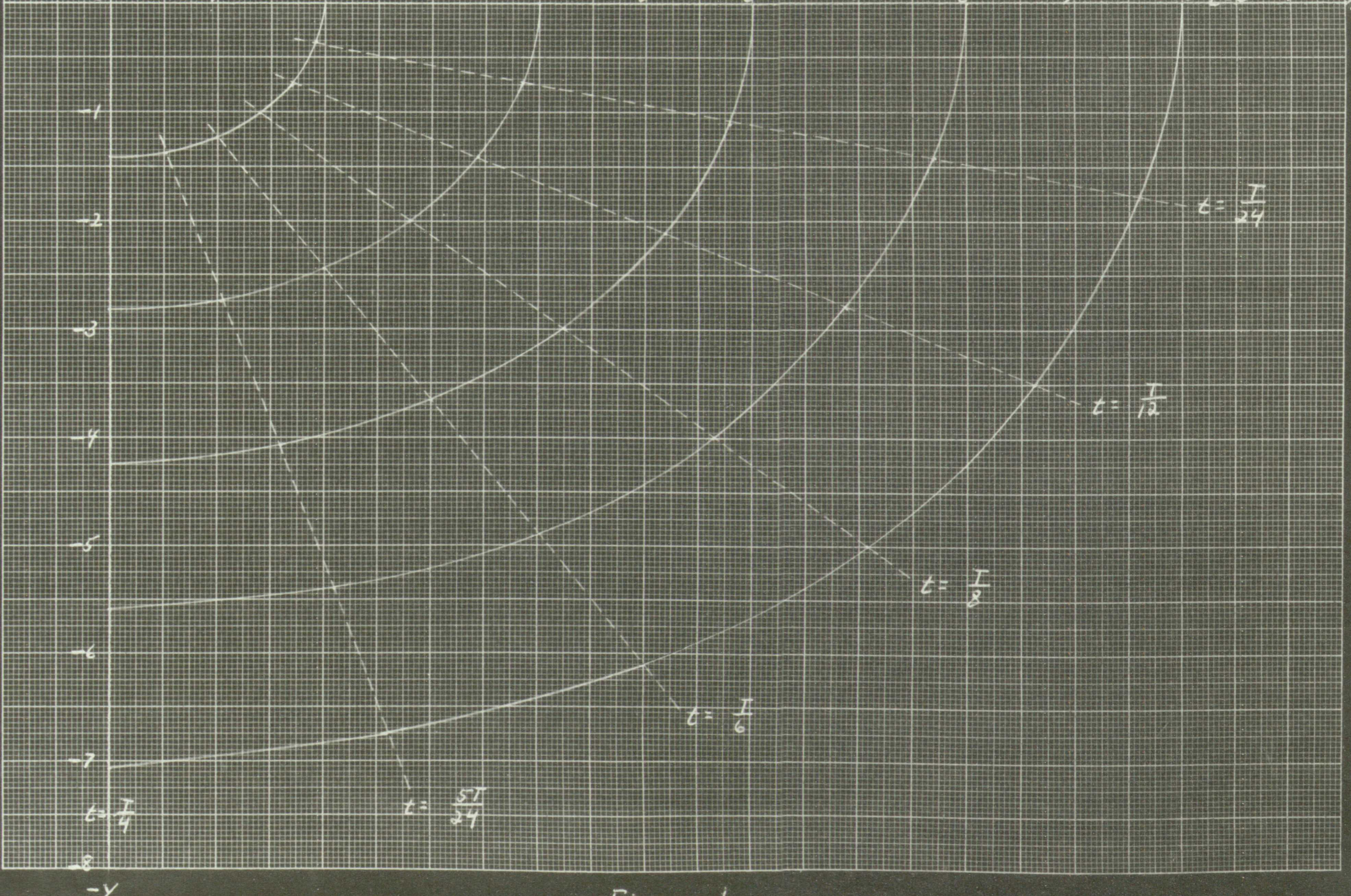

Figure 1

Equations (32) then constitute the Lagrangian description of $\vec{\tilde{P}}$. For purposes of calculation a P-whirlring centered initially about the point (10,0) was chosen with the functional form

$$\left|\vec{\tilde{P}}^{o}\right| = r e^{-\frac{r^2}{\delta^2}} \tag{33}$$

where r is the radial coordinate from the center of the whirlring and δ is a constant chosen to insure the scale of $\vec{P}$ to be small compared to the scale of $\vec{Q}_o$. For this specific calculation the components of $\vec{\tilde{P}}$ were taken as

$$\tilde{P}_x^{o} = -y^{o}\, e^{-\frac{2[(x^{o}-10)^2+y^{o2}]}{L^2}} \; ; \; \tilde{P}_y^{o} = (x^{o}-10)\, e^{-\frac{2[(x^{o}-10)^2+y^{o2}]}{L^2}} \tag{34}$$

where L is the scale of $\vec{\tilde{P}}$. Substitution of equations (34) into (32) yields

$$\tilde{P}_x = \left[-y^{o}\cos\sqrt{bc_1}\,t + (x^{o}-10)\sqrt{\tfrac{b}{c_1}}\sin\sqrt{bc_1}\,t\right] e^{-2[(x^{o}-10)^2+y^{o2}]}$$

$$\tilde{P}_y = \left[y^{o}\sqrt{\tfrac{c_1}{b}}\sin\sqrt{bc_1}\,t + (x^{o}-10)\cos\sqrt{bc_1}\,t\right] e^{-2[(x^{o}-10)^2+y^{o2}]} \; . \tag{35}$$

Of particular interest is the change of the shape of the $\vec{P}$-ring with time. The results for motion through one quadrant are shown in figure 2. The $\vec{Q}_o$-flow though not shown is the same as in figure 1. Further, all concentric $\vec{\tilde{P}}$-rings at $t=0$ will change with time like that depicted in figure 2. Note, the magnitude of $\vec{\tilde{P}}$ for a particular $\vec{\tilde{P}}$-ring is not preserved with time. This is illustrated in figure 3 where the magnitude of $\vec{\tilde{P}}$ for a few representative points on the initial ring is plotted against time. It is seen that the values of $|\vec{\tilde{P}}|$ remain small compared to those of $|\vec{Q}_o|$ throughout the motion; the same is true of its scale length.

Equations (32) then constitute the Lagrangian description of $\vec{F}$. For purposes of calculation a $\vec{F}$-whirlring centered initially about the point (10,0) was chosen with the functional form

$$|\vec{F}| = r e^{-\frac{r^2}{\delta^2}} \qquad (33)$$

where r is the radial coordinate from the center of the whirlring and δ is a constant chosen to insure the scale of $\vec{F}$ to be small compared to the scale of $\vec{\Omega}_0$. For this specific calculation the components of $\vec{F}$ were taken as

$$F_x^0 = -y^0 e^{-\frac{2[(x^0-10)^2+y^{0\,2}]}{L^2}}, \quad F_y^0 = (x^0-10) e^{-\frac{2[(x^0-10)^2+y^{0\,2}]}{L^2}} \qquad (34)$$

where L is the scale of $\vec{F}$. Substitution of equations (34) into (32) yields

$$F_x = \left[-y^0 \cos\sqrt{\Omega_0}\,t + (x^0-10)\sqrt{\tfrac{\Omega_0}{\Omega_0}} \sin\sqrt{\Omega_0}\,t\right] e^{-\frac{2[(x^0-10)^2+y^{0\,2}]}{L^2}}$$

$$F_y = \left[y^0\sqrt{\tfrac{\Omega_0}{\Omega_0}} \sin\sqrt{\Omega_0}\,t + (x^0-10)\cos\sqrt{\Omega_0}\,t\right] e^{-\frac{2[(x^0-10)^2+y^{0\,2}]}{L^2}} \qquad (35)$$

Of particular interest is the change of the shape of the $\vec{F}$-ring with time. The results for motion through one quadrant are shown in Figure 7. The $\vec{\Omega}_0$-flow though not shown is the same as in Figure 1. Further, all concentric $\vec{F}$-rings at $t=0$ will change with time like that depicted in Figure 8. Note, the magnitude of $\vec{F}$ for a particular $\vec{F}$-ring is not preserved with time. This is illustrated in Figure 3 where the magnitude of $\vec{F}$ for a few representative points on the initial ring is plotted against time. It is seen that the values of $|\vec{F}|$ remain small compared to those of $|\vec{\Omega}_0|$ throughout the motion; the same is true of its scale length.

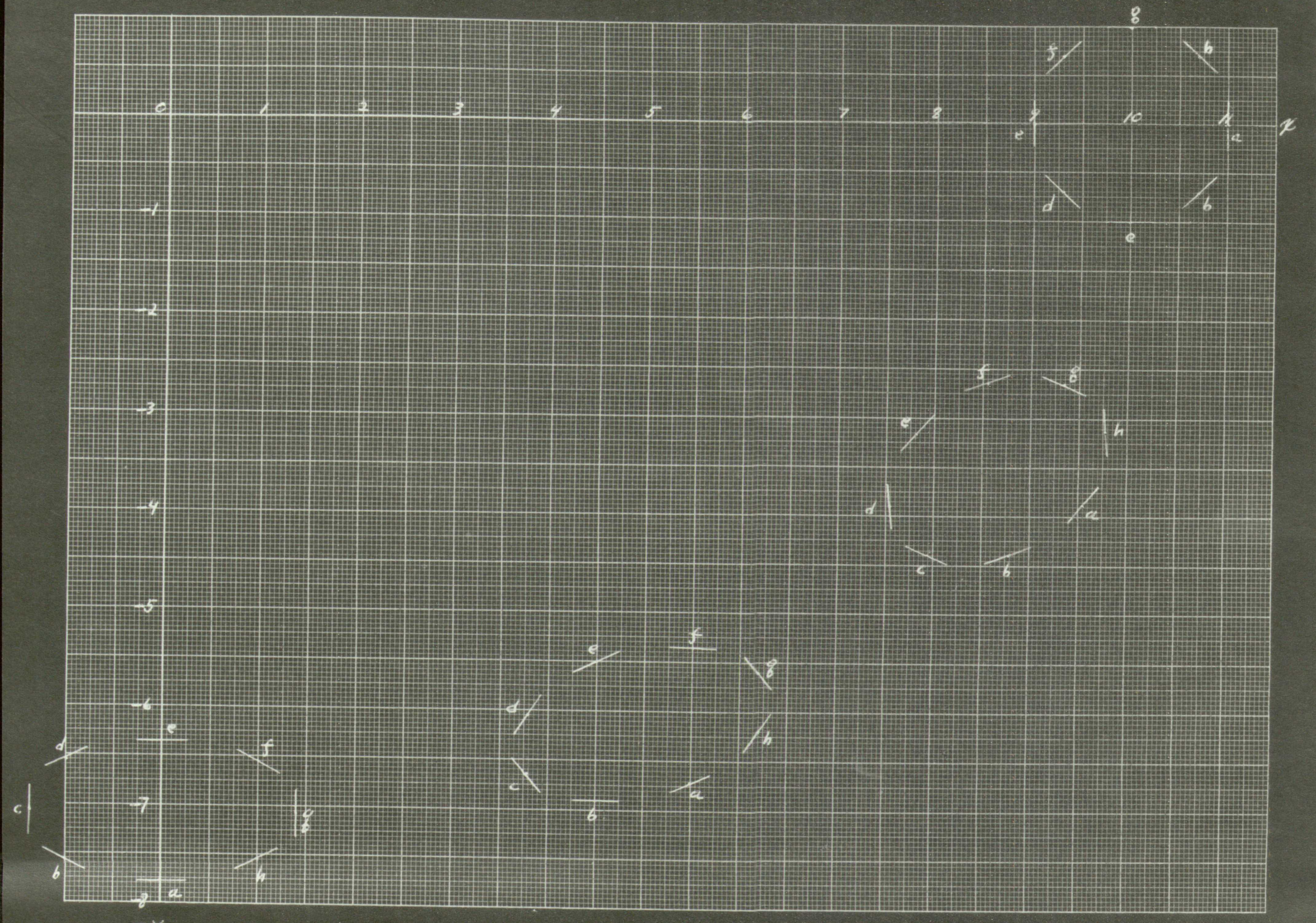

Figure 2

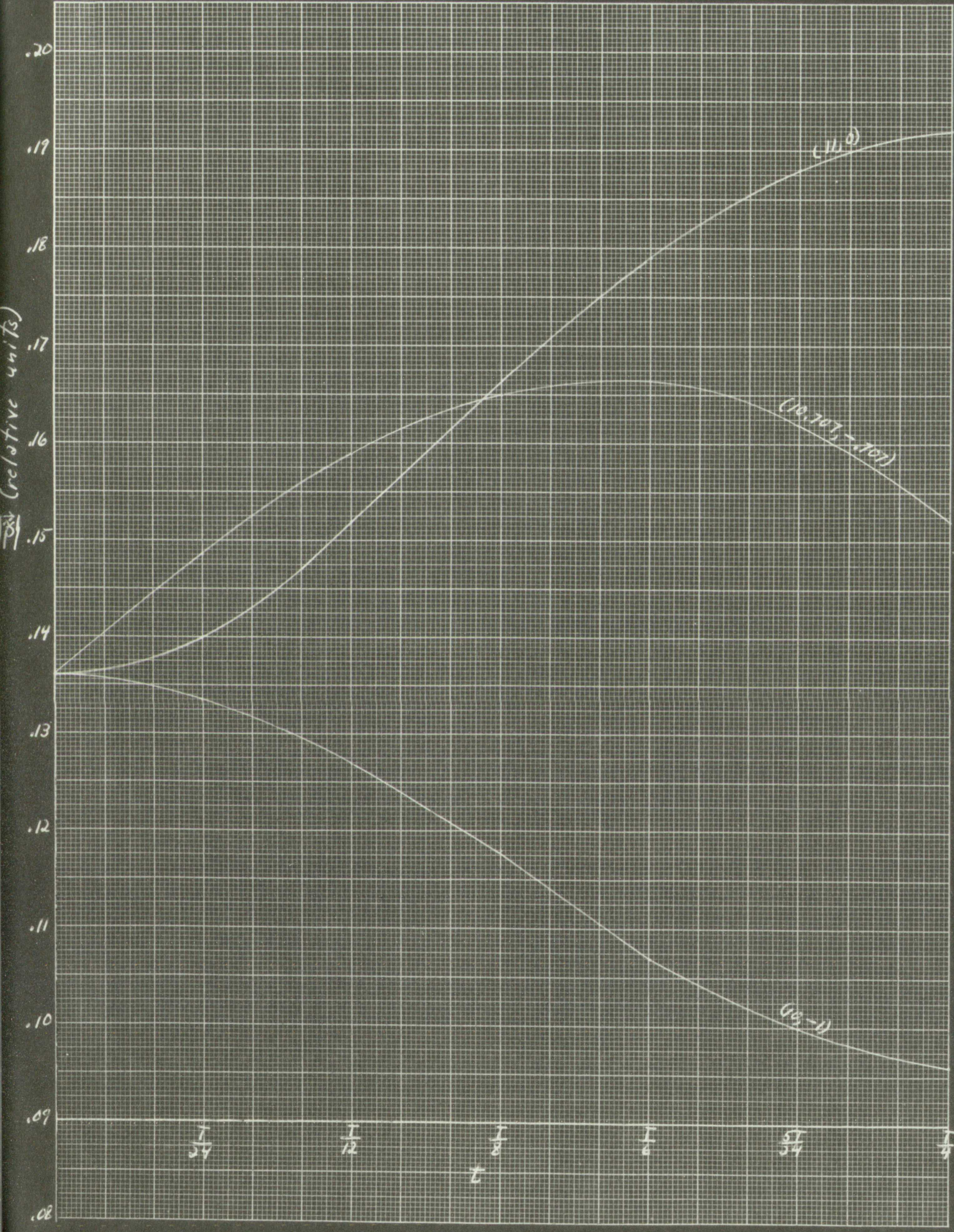
(relative units)
.20
.19
.18
.17
.16
.15
.14
.13
.12
.11
.10
.09
.08
T/24
T/12
T/8
T/6
5T/24
T/4
t

Figure 3

To investigate the hyperbolic case we return to equation (16), the general conic

$$\frac{c}{2}x^2 - \frac{b}{2}y^2 - axy + K_2 x - K_1 y + e = 0$$

in which we demand

$$a^2 + bc > 0. \tag{36}$$

To insure this condition we let

$$a = 0,\ b > 0,\ c > 0 \tag{37}$$

and for convenience we again let $K_1 = K_2 = 0$. Under these conditions the equations of motion for the Q_o-fluid take on the form

$$x = \sqrt{\frac{b}{c}}\, y^o \sinh \sqrt{bc}\, t + x^o \cosh \sqrt{bc}\, t$$

$$y = y^o \cosh \sqrt{bc}\, t + \sqrt{\frac{c}{b}}\, x^o \sinh \sqrt{bc}\, t. \tag{38}$$

These equations are the parametric equations for a family of hyperbolae as can be seen by forming

$$\frac{y^2}{y^{o2} - \frac{c}{b} x^{o2}} - \frac{x^2}{\frac{b}{c}\left[y^{o2} - \frac{c}{b} x^{o2}\right]} = 1. \tag{39}$$

These hyperbolae have an eccentricity, $e = \sqrt{1 + b/c}$, and are bounded by the asymptotes, $y = \pm\sqrt{\frac{c}{b}}\,x$. The flow for representative points initially on the positive x axis is depicted in figure 4; the times are in terms of T, the period in the comparable elliptical case. Here a ratio of $\frac{b}{c} = \frac{1}{6}$ was chosen for calculation purposes. From figure 4 we see how rapidly the velocity, i.e. Q_o, varies along a particular streamline. As our expansion demands, it is proportional to the distance from the origin; in this calculation the y

To investigate the [illegible] equation (46), the [illegible]

$$[illegible]$$

in which we [illegible]

$$a^2 + 4c > 0$$

To insure this condition [illegible]

$$a = 0, \ldots$$

and for convenience [illegible] conditions the equation [illegible] on the form

$$[illegible]$$

$$[illegible]$$

These equations [illegible] of hyperbolas [illegible]

$$[illegible]$$

These hyperbolas have [illegible] bounded by the [illegible] ative points [illegible] in figure [illegible] component [illegible] for calculation [illegible] the velocity, [illegible] line. [illegible] the distance [illegible]

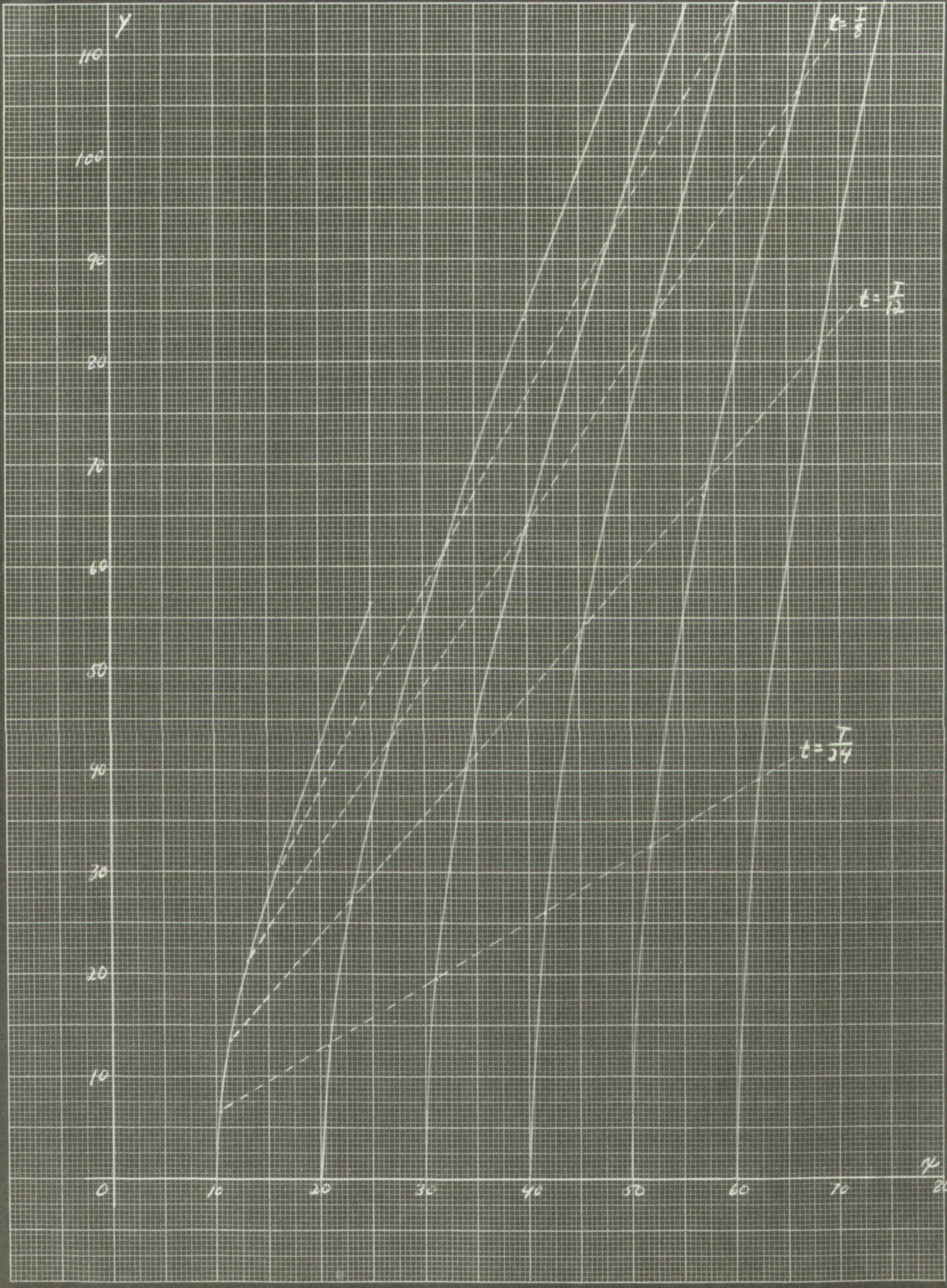
y
110
100
90
80
70
60
50
40
30
20
10
0
10
20
30
40
50
60
70
φ
t = T/8
t = T/12
t = T/24

Figure 4

component of $\vec{Q}_o$ dominates the x component due to the ratio chosen and also due to the fact that our initial points are along the x axis.

Figures 5,6,7,8, and 9 show then the effect of this hyperbolic flow on a $\vec{P}$-ring of the same functional form as in the elliptical case, but centered initially at (25,0). The equations for P in this case are

$$\tilde{P}_x = \left[-y^\circ \cosh \sqrt{6c}\,t + \sqrt{\tfrac{1}{6}}\,(x^\circ - 25) \sinh \sqrt{6c}\,t \right] e^{-2[(x^\circ-25)^2 + y^{\circ 2}]}$$

$$\tilde{P}_y = \left[-y^\circ \sqrt{6} \sinh \sqrt{6c}\,t + (x^\circ - 25) \cosh \sqrt{6c}\,t \right] e^{-2[(x^\circ-25)^2 + y^{\circ 2}]} \quad . \qquad (40)$$

Figure 10 shows the variation of the magnitude of $\vec{P}$ with time for a few representative points. In calculating these curves the common exponential damping factor was ignored; however, it can be seen that the variation in the amplitude of $\vec{P}$ is small compared to the amplitude of $\vec{Q}_o$. Also, the previous graphs show that the scale of $\vec{P}$ remains small compared to the scale of $\vec{Q}_o$ in accord with our previous assumptions.

Lastly a tabulation of the $\vec{P}$-ring tangents for these graphs is included.

component of $\vec{\xi}_y$ calculates the x component due to the field chosen and also due to the fact that our initial points are along the x-axis.

Figures 7,8,9, and 9 show then the effect of this hyperbolic flow on a $\vec{\xi}$-ring of the same functional form as in the elliptical case, but centered initially at (25,0). The equations for $\vec{\xi}$ in this case are:

$$\xi_x = \left[y \cos\sqrt{[illegible]}\,t + \sqrt{[illegible]}\,(x-25)\sin\sqrt{[illegible]}\,t \right] e^{-2[(x-25)^2 + y^2]}$$

$$\xi_y = \left[-y \sqrt{[illegible]}\,\sin\sqrt{[illegible]}\,t + (x-25)\cos\sqrt{[illegible]}\,t \right] e^{-2[(x-25)^2 + y^2]} \quad (10)$$

Figure 10 shows the variation of the magnitude of $\vec{\xi}$ with time for a few representative points. In calculating these curves the common exponential damping factor was ignored; however, it can be seen that the variation in the amplitude of $\vec{\xi}$ is small compared to the amplitude of $\vec{\xi}_0$. Also, the previous graphs show that the scale of $\vec{\xi}$ remains small compared to the scale of $\vec{\xi}_0$ in accord with our previous assumptions.

Lastly a tabulation of the $\vec{\xi}$-line tangents for these graphs is included.

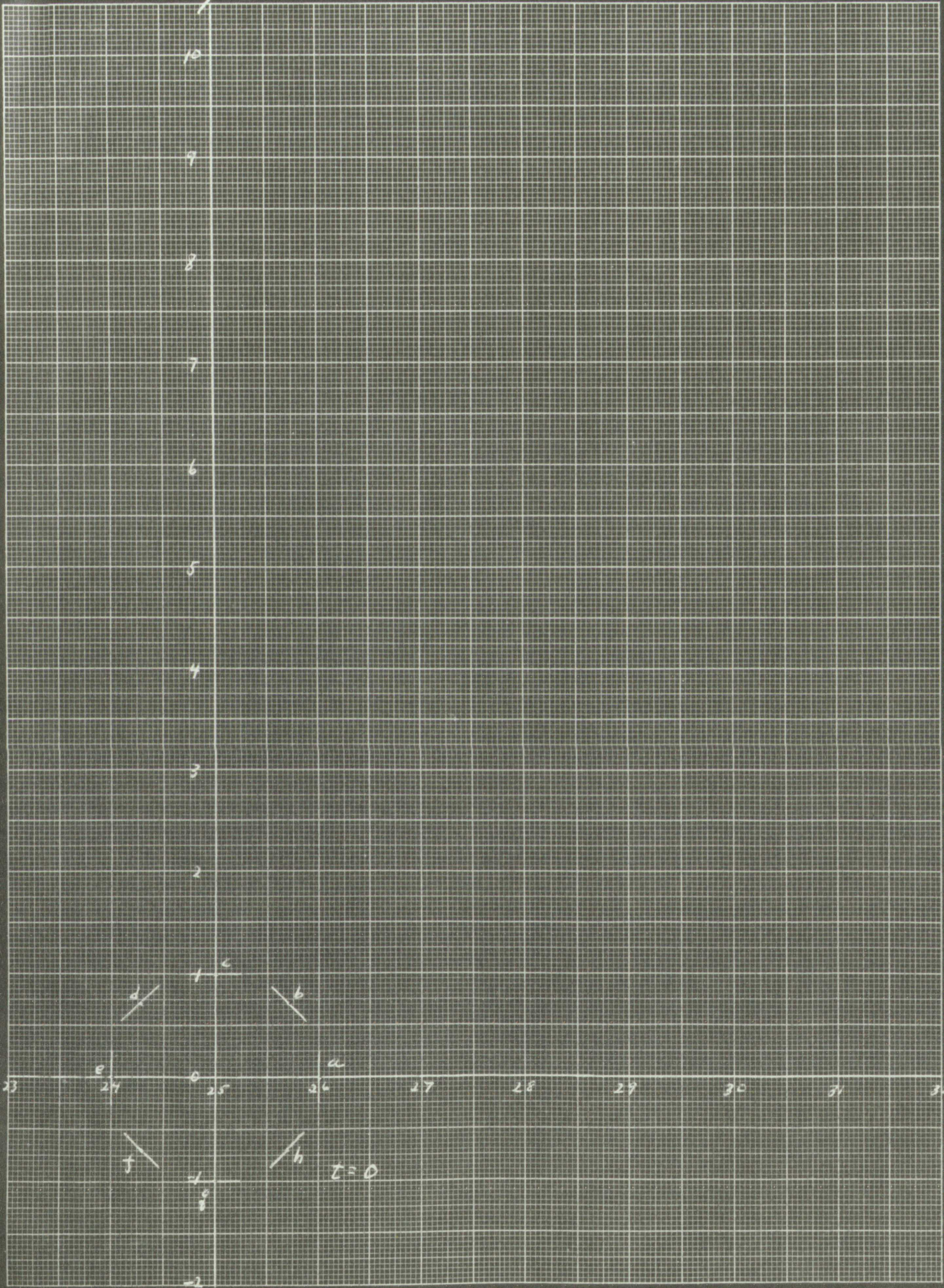

Figure 5


21
20
19
18
17
16
15
14
13
12
11
b
c
a
d
h
e
g
f
t = T/24

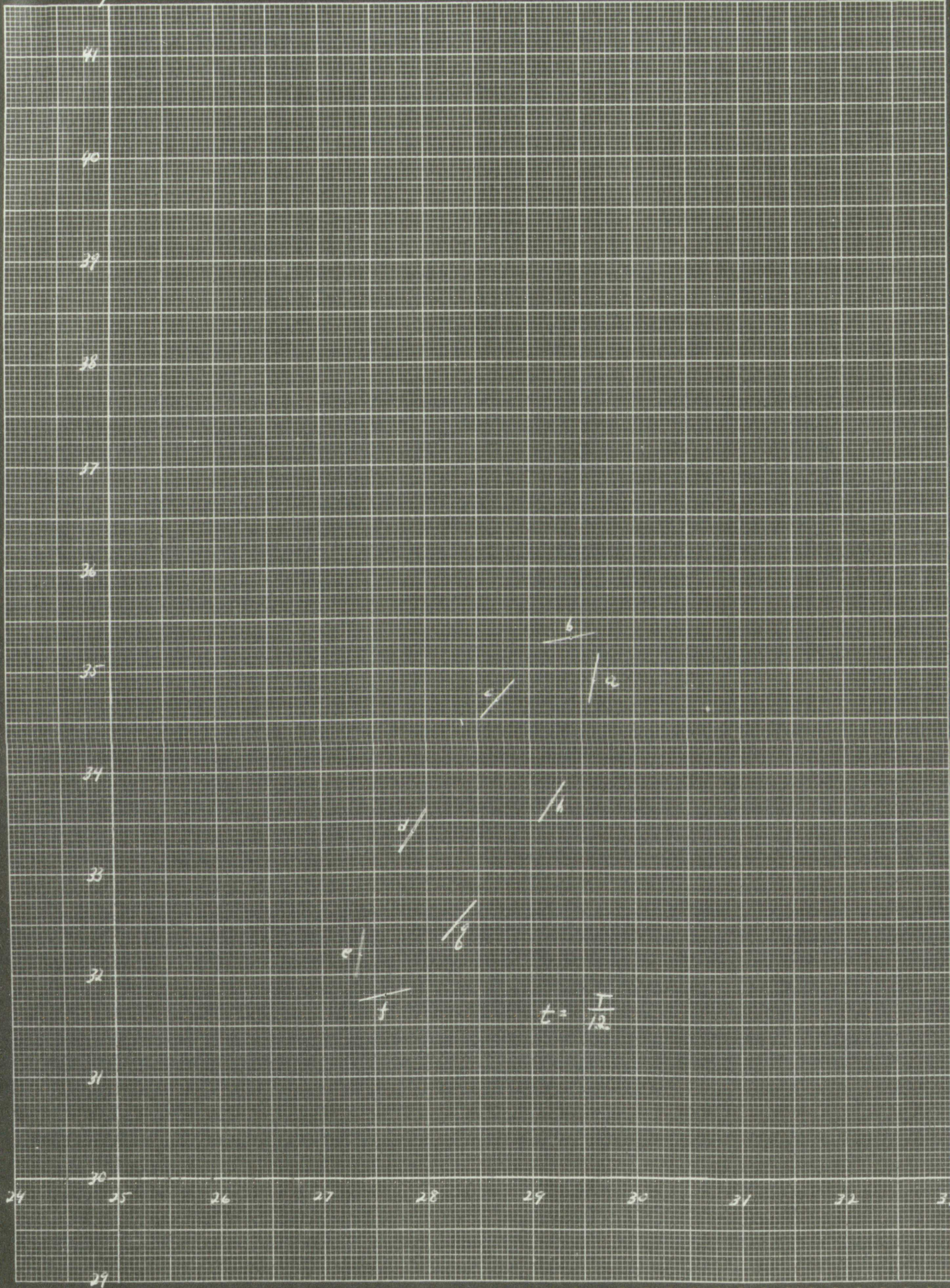

41
40
39
38
37
36
35
34
33
32
31
30
29
24
25
26
27
28
29
30
31
32
a
b
c
d
e
f
g
h
$t = \frac{T}{12}$

Figure 7

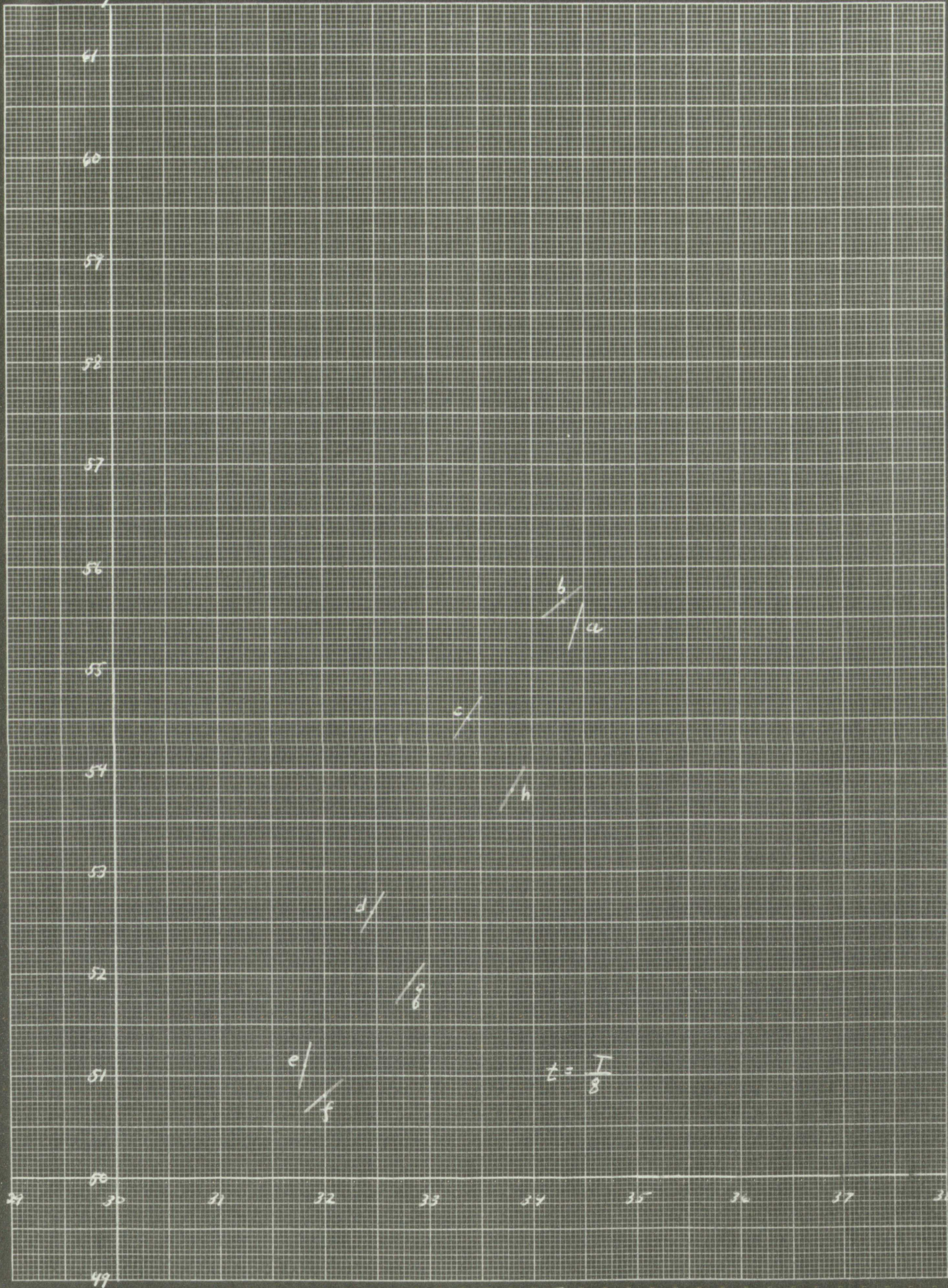

Figure 8

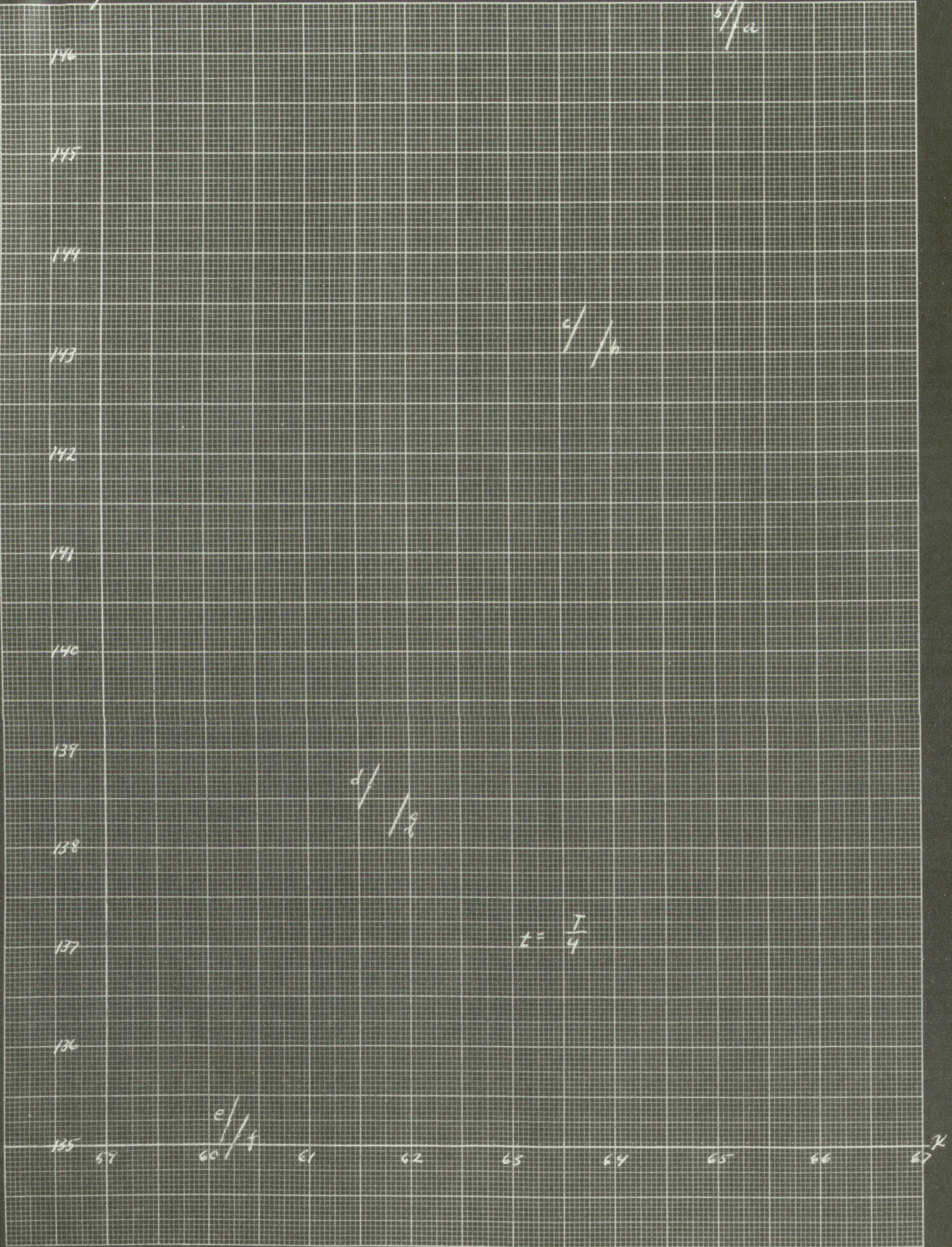

146
145
144
143
142
141
140
139
138
137
136
135
59
60
61
62
63
64
65
66
67
x
a
b
c
d
e
f
g
h
t = T/4

Figure 9

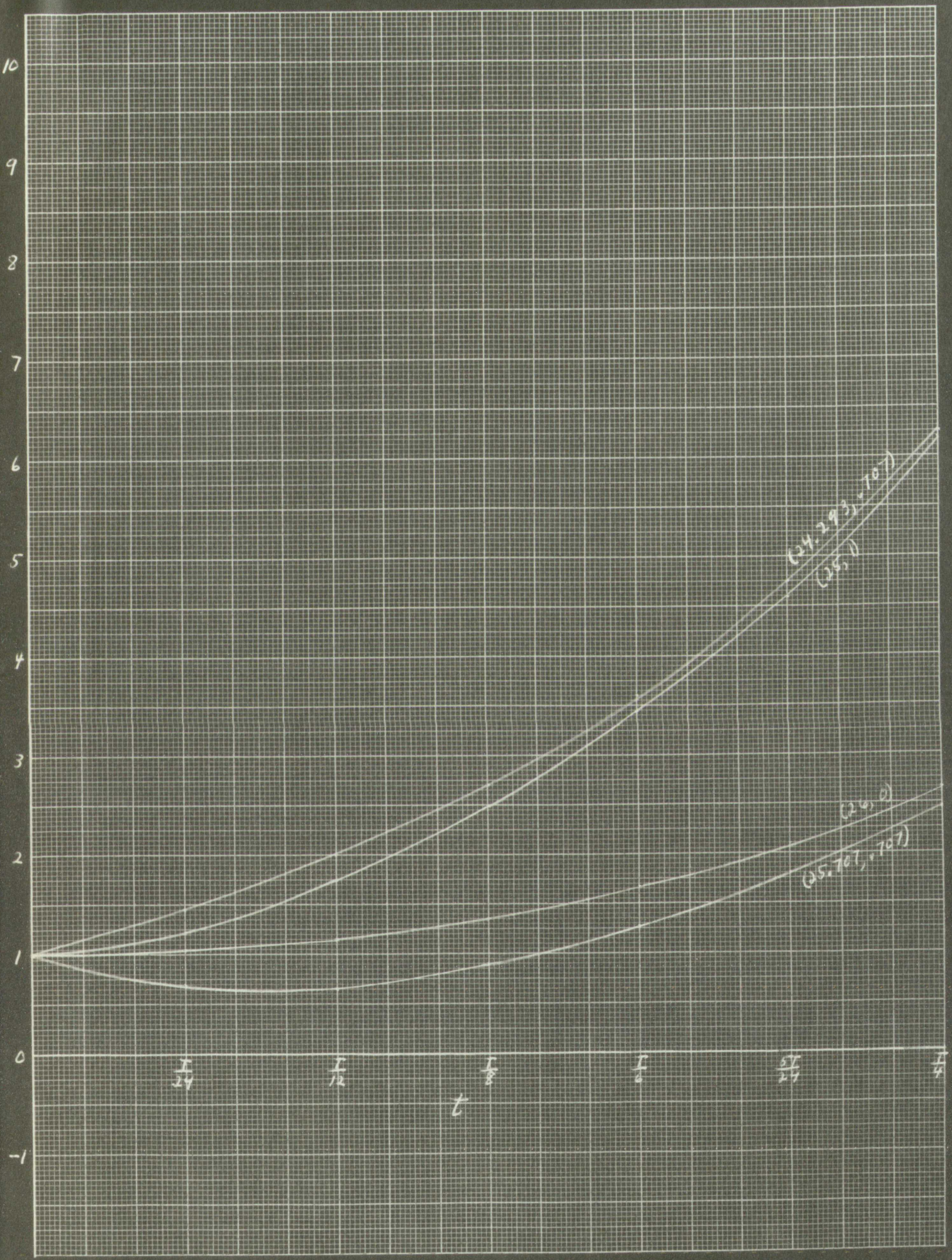

10
9
8
7
6
5
4
3
2
1
0
-1
(24.293, .707)
(25, 1)
(26, 0)
(25.707, .707)
π/24
π/12
π/8
π/6
5π/24
π/4
t

Figure 10

Table 1

P-ring Tangents

1. elliptical case, figure 4

point		time		
	0	T/12	T/6	T/4
a.	∞	1.23	0.410	0.00
b.	1.00	0.326	-0.066	-0.50
c.	0.00	-0.408	-1.23	∞
d.	-1.00	-7.60	1.54	0.50
e.	∞	1.23	0.410	0.00
f.	1.00	0.326	-0.066	-0.50
g.	0.00	-0.408	-1.23	∞
h.	-1.00	-7.60	1.54	0.50

2. hyperbolic case, figures 5,6,7,8,9

	0	T/24	T/12	T/8	T/4
a.	∞	9.58	5.09	3.73	2.68
b.	-1.00	-0.411	0.216	0.830	1.98
c.	0.00	0.63	1.18	1.61	2.25
d.	1.00	1.48	1.82	2.06	2.37
e.	∞	9.58	5.09	3.73	2.68
f.	-1.00	-0.411	0.216	0.83	1.98
g.	0.00	0.63	1.18	1.61	2.25
h.	1.00	1.48	1.82	2.06	2.37